Angular Distribution of 424-Mev Polarized Protons Elastically Scattered from Various Nuclei*†

EDVARD HEIBERG‡
The Enrico Fermi Institute for Nuclear Studies, The University of Chicago, Chicago, Illinois
(Received March 1, 1957)

Measurements have been made of the polarization and the angular distribution of 424-Mev protons elastically scattered from carbon, aluminum, iron, and silver. The results clearly indicate the importance of separating the elastic scattering from scattering involving excited states of the nucleus. By the inclusion of inelastic scattering, the dips in the cross-section curves and the details in the polarization curves get smeared out. The carbon data show reasonable agreement with similar work by Chesnut. Elastic cross sections were estimated by extrapolating the differential cross-section curves to zero degrees using the optical model of the nucleus.

A nuclear radius was calculated from the location of the first diffraction minima in the cross section curves for the various elements. Upon using the optical model, an average value $r_0=1.03\times10^{-13}$ cm was obtained. The Born approximation gave $r_0=1.2\times10^{-13}$ cm.

I. INTRODUCTION

IN recent years, accelerator groups at the University of Rochester,[1,2] the University of California,[3] Harwell,[4,5] Carnegie Institute of Technology,[6] Harvard University,[7,8] Institute of Nuclear Problems, Moscow,[9] and at this University[10,11] have been engaged in studying polarization effects of nucleons scattered from various nuclei at energies above 50 Mev.

All these experiments were initiated when Oxley *et al.*,[1] in 1953, successfully measured polarization of about 200-Mev protons scattered from nuclei. It was then quickly realized that this technique could be developed into great precision, and would represent another important tool in unwrapping the complexity of nuclear forces.

The formalism, used in theoretical treatments of polarization, was developed by Wolfenstein.[12] The spin-orbit coupling, as the mechanism involved in high-energy polarization, was first employed by Fermi.[13] The nuclear shell model has since then been used for the same purpose by several authors.[14–27]

II. EXPERIMENTAL TECHNIQUE

A. General Considerations

Detailed reviews of high-energy polarization experiments are given in many papers, one of which is a recent survey of the Berkeley work.[3] Consequently, this section will only describe the technique of this experiment.

During the last year, it has become evident that in order to evaluate the mechanism of high-energy polarization, one must separate the effect of the elastic scattering from scattering into the excited states of the nucleus. This was clearly demonstrated by Chesnut in a recent report from Rochester.[2]

It is also important to work with high angular resolution. This requirement, together with a good

* Research supported by a joint program of the Office of Naval Research and the U. S. Atomic Energy Commission.

† Based on a thesis submitted to the Faculty of the Department of Physics, the University of Chicago, in partial fulfillment of the requirements for the Ph.D. degree.

‡ Present address: AB Atomenergi, Stockholm, Sweden.

[1] Oxley, Cartwright, Rouvina, Baskir, Klein, Ring, and Skillman, Phys. Rev. **91**, 419 (1953); see also Oxley, Cartwright, and Rouvina, Phys. Rev. **93**, 806 (1954).

[2] W. G. Chesnut, *Proceedings of the Sixth Annual Rochester Conference on High-Energy Nuclear Physics* (Interscience Publishers, Inc., New York, 1956); see also Chesnut, Hafner, and Roberts, Phys. Rev. **104**, 449 (1956).

[3] Chamberlain, Segrè, Tripp, Wiegand, and Ypsilantis, Phys. Rev. **102**, 1659 (1956). See also E. Segrè, Physica **22**, 1079 (1956).

[4] J. M. Dixon and D. C. Salter, Nature **173**, 946 (1954); Dixon, Rose, and Salter, Proc. Phys. Soc. (London) **A68**, 361 (1955); M. J. Brinkworth and B. Rose, Nuovo cimento **1**, 195 (1956).

[5] Report of Harwell work at the Amsterdam conference of nuclear physics, July, 1956. See J. M. Dickson, Physica **22**, 1172 (1956); T. H. R. Skyrme, Physica **22**, 1179 (1956).

[6] Kane, Stallwood, Sutton, Fields, and Fox, Phys. Rev. **95**, 1694 (1954); Siegel, Hartzler, and Love, Phys. Rev. **101**, 838 (1956).

[7] K. Strauch, Phys. Rev. **98**, 234 (1955); **99**, 150 (1955).

[8] K. Strauch, University of California Radiation Laboratory Report UCRL-3211, November 1955 (unpublished).

[9] Report of Russian work at the Amsterdam conference of nuclear physics, 1956. See I. I. Levintov, Physica **22**, 1178 (1956); L. N. Rosenzweig, Physica **22**, 1179 (1956).

[10] Marshall, Marshall, Nagle, and Skolnik, Phys. Rev. **95**, 1020 (1954).

[11] Marshall, Marshall, and de Carvalho, Phys. Rev. **93**, 1431 (1954); de Carvalho, Marshall, and Marshall, Phys. Rev. **96**, 1081 (1954); Heiberg, Kruse, Marshall, Marshall, and Solmitz, Phys. Rev. **97**, 250 (1955); L. Marshall and J. Marshall, Phys. Rev. **98**, 1398 (1955).

[12] L. Wolfenstein, Phys. Rev. **75**, 1664 (1949).

[13] E. Fermi, Nuovo cimento **11**, 407 (1954); exact calculation privately communicated.

[14] W. Heckrotte and J. V. Lepore, Phys. Rev. **94**, 500 (1954).

[15] Snow, Sternheimer, and Yang, Phys. Rev. **94**, 1073 (1954).

[16] W. Heckrotte, Phys. Rev. **94**, 1797 (1954).

[17] B. J. Malenka, Phys. Rev. **95**, 522 (1954).

[18] I. I. Levintov, Doklady Akad. Nauk (U.S.S.R.) **98**, 373 (1954).

[19] E. Bosco and T. Regge, Nuovo cimento **12**, 285 (1954).

[20] R. Sternheimer, Phys. Rev. **95**, 587 (1954); **97**, 1314 (1955); **100**, 886 (1955).

[21] Fernbach, Heckrotte, and Lepore, Phys. Rev. **97**, 1059 (1955).

[22] R. Wilson, Phil. Mag. **46**, 769 (1955).

[23] A. Sjölander and S. Köhler, Arkiv Fysik **8**, 521 (1954).

[24] S. Köhler, Nuovo cimento **2**, 911 (1955).

[25] T. Eriksson, Nuovo cimento **2**, 907 (1955).

[26] T. Eriksson and W. J. Swiatecki, Arkiv Fysik **9**, 281 (1955).

[27] W. Heckrotte, Phys. Rev. **101**, 1406 (1956).

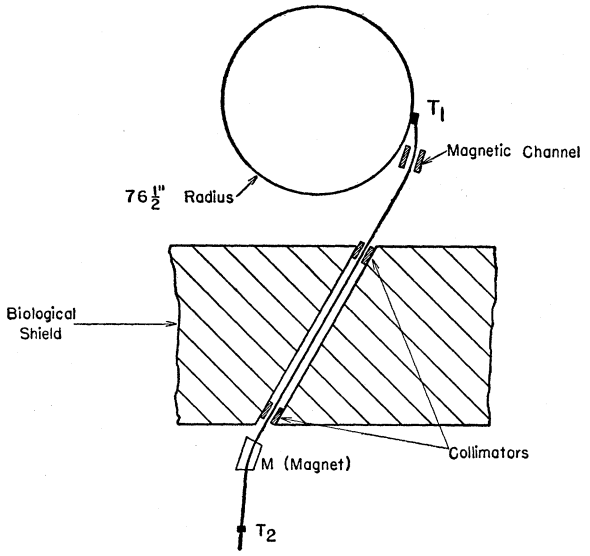

FIG. 1. Plan view of the 460-Mev synchrocyclotron area showing the experimental setup used to produce a 424 Mev, 54% polarized proton beam.

energy resolution, enables one to observe strong dips in the cross-section curves as a function of scattering angle, and corresponding large variations in the polarization curves.

Chesnut[2] has shown that a scattering process leading to the first excited state in carbon, tended to fill out the dip in the polarization curve observed in the scattering from the ground state. This work has followed in the general direction of the Rochester pattern.

Because of straggling and spread in the energy of the proton beam, it was not feasible to make a complete separation of the elastic effects from the inelastic. The results, however, indicate the importance of good energy resolution by which the contribution of the various excited states can be excluded.

B. Double Scattering

The conventional double-scattering technique was used.[1] Accordingly, the polarization was determined by asymmetry measurements by the well-known relationship:

$$\epsilon=(L-R)/(L+R)=P_iP_j, \qquad (1)$$

where ϵ is the asymmetry, L and R are counting rates corrected for backgrounds at equal scattering angles to the left and to the right, and P_i is the initial polarization of the beam, which in the present experiment was measured to be $(53.5\pm0.9)\%$. This was done in the usual way.[10] The quantity P_j is the polarization produced in an unpolarized beam by scattering from the target.

The target in which the first scattering occurred (specified as T_1 in Fig. 1), was a $\frac{1}{2}$ in.$\times\frac{1}{2}$ in.$\times1$ in. beryllium slab, located with one of its diagonal planes in the median plane of the cyclotron. The 1-in. target edge was mounted parallel with the trajectory of the clockwise rotating beam hitting it, and placed at a distance of $76\frac{1}{2}$ in. from the center of the magnet. A magnetic channel, designed by U. E. Kruse of this Institute, was placed in the vacuum tank in such a way that particles scattered 10° left from the target, would be deflected out through an evacuated pipe directly connected with the cyclotron vacuum through the biological shield wall into the experimental area. Figure 1 gives a general idea of this arrangement.

At both ends of the evacuated pipe, brass collimators were inserted. The dimensions of the collimator at the cyclotron side of the shield were 1-in. (width)$\times$2 in. (height)$\times$7 in. (length). The corresponding dimensions of the collimator at the experimental area side of the shield were 2 in.$\times1\frac{3}{4}$ in.$\times$7 in. This latter collimator was pushed about $3\frac{1}{2}$ ft inside the shield wall to avoid producing too large a neutron background in the experimental pit from reactions in the collimator. The widths and the positions of the collimators were adjusted to take into account the divergence of the beam determined by x-ray film exposures.

An analyzing magnet (M) with a 3-in. gap deflected the beam about 26° in the experimental area. An ionization chamber, placed before the second scatterer (T_2), was used as a monitor. From the end of the evacuated pipe to the ionization chamber, the beam passed through a thin bag filled with helium in order to reduce the air scattering. A general layout of the counter telescope is given in Fig. 2.

The approximate height and width of the beam hitting the second target were photographically determined to be 1 in. and $1\frac{1}{2}$ in. As the targets used were narrower than the beam hitting them, the total geometrical angular resolution of this system was determined by the width of the target, the width of the defining counter in the telescope, and the angular spread of the beam.

C. Counter Telescope

The telescope consisted essentially of four counters connected in various coincidence arrangements. The counters are numbered 1, 2, 3, and 4 in Fig. 2. Counter 2 was the defining counter and placed 48.5 in. from the target. Counter 1 was put as close to the target as possible without being hit by the beam at the smallest scattering angles measured. A reduction in the chance

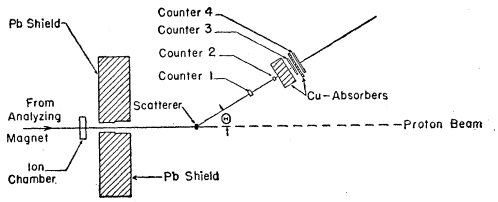

FIG. 2. Geometry for the second scattering. Arrangement of the monitor, the scattering telescope, and the shielding.

coincidence backgrounds was achieved, by putting counters 1 and 2 as far apart as possible. Counters 3 and 4 have large areas, and are behind different amounts of copper absorbers. Thus, two angular distribution curves can be recorded simultaneously, one containing more inelastic contamination than the other. A further description of the counters and the associated electronics is given below in Sec. II E.

The angles were changed by means of a swivel arrangement, and in this way, the relative angular positioning of the telescope was fixed within 1/50 of a degree.

D. Monitoring

For monitoring purposes, a 6-in. diameter ionization chamber, designed by H. Kobrak of this Institute, was used. The total thickness of the aluminum walls was 0.006 in., and the gauge pressure of the argon gas was 5 lb/in.^{2}. The electron collector plate of the chamber was connected to a condenser parallel to a vibrating reed circuit. When the condenser was charged to a certain preset potential difference, the cyclotron was automatically turned off. The reproducibility of this system was about 1%.

E. Electronics

Plastic scintillators were used as detectors. The light pipes, depending on the application of the counter, were either of air or Lucite, and connected the plastic optically to RCA type 5819 photomultiplier tubes. The air light pipe was designed as follows.

Thin aluminum foil was wrapped around the scintillating plastic and extended as a hollow shaft down to the cathode of the photomultiplier tube. The loss of the light intensity hitting the cathode was substantially reduced by reflections on the aluminum foil. This arrangement, as used for counters 1 and 2, had the feature that no pulses caused by Čerenkov light could be produced. Table I gives the dimensions of the counters used.

The 5819 tubes were selected so that they all could be operated from the same power supply. By operating the last dynode essentially at anode potential of each photomultiplier, a space charge effect was obtained which limited the size of the output pulses.[28] These pulses were appropriately amplified by a chain of distributed amplifiers, and then fed through adjustable delay units into a cut-off diode coincidence circuit designed by J. Fischer of this Institute. Here the pulses were "clipped" by four millimicroseconds long, shorted transmission lines, which determined the resolving time of the coincidence circuit ($\sim 10^{-8}$ sec).

TABLE I. Specifications of the counters employed in the telescope. Dimensions are in inches. All the counters were made of scintillating plastic $\frac{1}{4}$ in. Counter 2 was the defining counter.

Counter	Width	Height
1	1	4
2	$\frac{3}{4}$	3
3	3	5
4	4	6

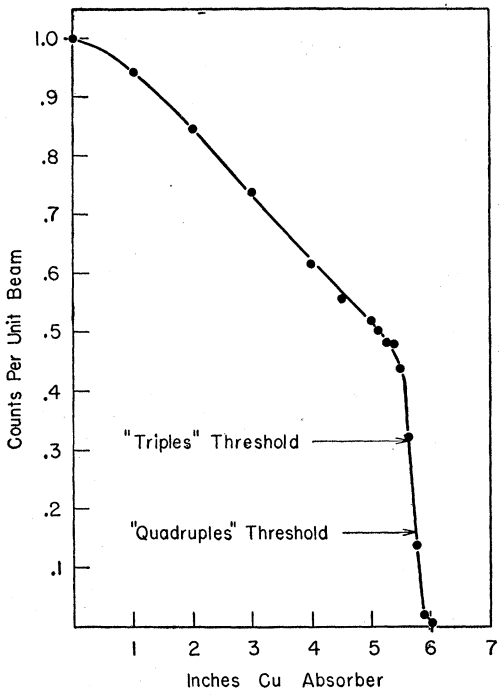

FIG. 3. Range curve to determine the energy of the beam and the thresholds of the telescope.

The coincidences made were "doubles" (1,2), "triples" (1,2,3), and "quadruples" (1,2,3,4). The various coincidence pulses were fed through corresponding amplifiers into their respective scalers. The delays, the voltage of the photomultipliers, and the attenuation of the coincidence pulses were adjusted, so that the system was working in the middle of plateaus with reasonable widths as previously reported.[10,29]

When the telescope was put in the direct beam with no copper between any of the counters, it was found that the counting rates were essentially the same for all the coincidences. During the recording of the data, the counting rate losses in the scalers could be neglected for both the triple and the quadruple counts at all scattering angles. This is because the intensity of these beams was so low.

The double counts gave a sensitive indication of the stability of the beam. It was observed, for example, that small fluctuations in the magnetic field of the analyzing magnet, gave corresponding variations in the counting rates of the "doubles." This was not noticed in the "triples" or the "quadruples."

[28] J. Fischer (private communication).

[29] H. G. de Carvalho, Phys. Rev. **96**, 398 (1954).

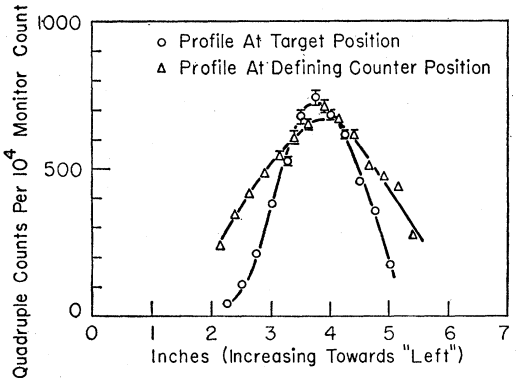

FIG. 4. Profile curves of the "quadruples" beam at the target position respectively the defining counter position, 48.5 in. apart from each other.

F. Lineup Procedure

The accuracy with which the polarization can be determined for the various elements, greatly depends on the precision of the lineup of the scattering table. This could be done to within $\pm 0.07°$. The details of the procedure will now be given.

In order to study elastic scattering, it is as previously indicated, necessary to discriminate against inelastic scattering. One way of achieving this, is to set the energy threshold of the telescope as high as possible, consistent with getting reasonable counting rates. The thresholds of the "triples" and the "quadruples" telescopes are given in Fig. 3.

It was estimated that the intensity of the beam hitting the second target was about 10^5 protons/cm^2/sec. This intensity was much too high for use of scintillation counters in the direct beam. A "clipper" designed by U. E. Kruse of this Institute, was lowered down into the beam quite near the center of the cyclotron. Any desired intensity reduction of the maximum beam could in this way be achieved. The assumption was then made that the center of gravity and the energy of the beam was not altered by this procedure. Accordingly, a lineup and an energy determination with the counter telescope in the direct reduced beam could be undertaken.

The center line of the scattering table was aligned with the center of gravity of the "quadruples" beam. By taking profile curves with the defining counter in its normal position, and at the target position, the results indicated in Fig. 4 were obtained. On the basis of these curves, the "quadruples" beam was estimated to be $\pm 0.6°$ divergent. Taking similar curves for the "triples" beam, it was found that this beam was 0.1° to the left of the "quadruples" beam. A corresponding correction had to be made to the "triples" data.

During the run, the lineup was occasionally checked, and the beam was found to fluctuate about $\pm 0.06°$. This fluctuation was probably due to variations in the analyzing magnet current, which was (750 ± 2) amp. By adjusting the current to 770 amp, and recording the equivalent change of the beam direction, the above variation corresponded to an angular fluctuation of 0.6°. This gives good agreement with the observed value.

III. ENERGY OF BEAM, THRESHOLDS OF TELESCOPE

A final range curve of the proton beam was taken after the lineup procedure, as shown in Fig. 3. The energy of the beam hitting the second target was

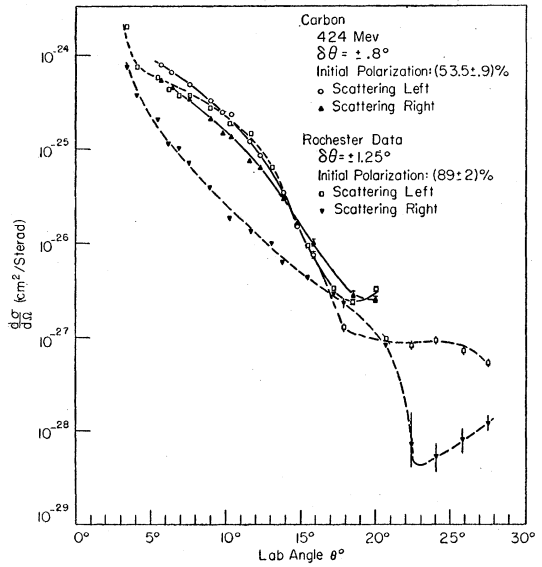

(a)

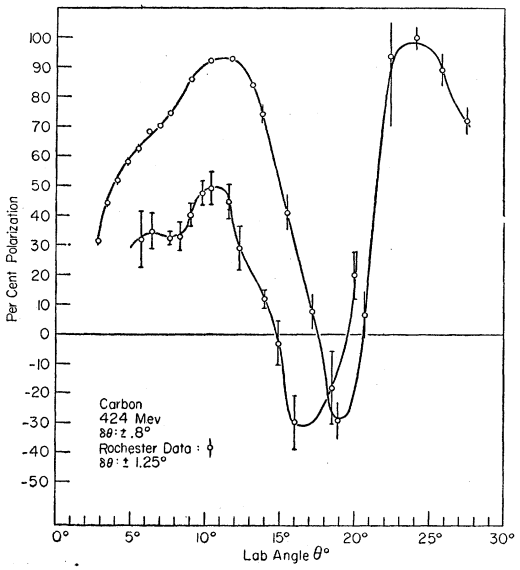

(b)

FIG. 5. (a) Differential cross-section curves for left and right scattered 424-Mev protons from carbon. Comparison with Rochester (Chesnut) data scaled from 220 Mev. (b) Corresponding polarization curve for 424-Mev protons scattered from carbon. Comparison with Rochester (Chesnut) data scaled from 220 Mev.

(424±5) Mev.[30] A correction for the total thickness of counters 1 and 2 was made.

The energy thresholds of the "quadruples" and "triples" counter telescopes were set to (426±3) Mev and (420±3) Mev, respectively.

IV. DATA

A. Measurements

Table II summarizes the polarization and the cross section measurements for carbon, aluminum, iron, and silver. Figures 5(a) and 5(b), 6(a) and 6(b), 7(a) and 7(b), 8(a) and 8(b) give the curves of these data. The (a)'s represent the cross section measurements and the (b)'s the corresponding polarization values. Chesnut's[2] 220-Mev data for carbon has been plotted in Figs. 5(a) and 5(b), and has been scaled to 424 Mev according to the ratio of the De Broglie wavelengths. The energy threshold of the telescope was always the same within ±0.5 Mev, and corrections for recoil energy losses in the second target were made.

The recorded errors are based on the variance of the number of counts from measurement to measurement, and not on the counting statistics as usually is done with this kind of data. The reason for this was fluctuations in the beam. With the geometry used, these variations were larger than one would expect from counting statistics alone. For this purpose at each angle, five to six separate recordings were made on each side of the beam. By calculating the variance for each set of measurements, the random error introduced by the fluctuations in the beam and also in the monitoring, were automatically included.

During the run, the consistency of the results was checked as follows. For a given element, the scattering at a series of angles was to be investigated. In the case of carbon, for example, the scattering angles were, 5.7°, 6.4°, 7.6°, 8.3°, 9.0°, 9.8°, etc. The data were first recorded at each second angle starting with 5.7°, then 7.6°, 9.0°, and so on. When this cycle was completed, the measurements at the intermediate angles 6.4°, 8.3°, 9.8°, etc., were done. Without any exception, the latter values fell between the first ones on a smooth curve.

During the two-week run, the air humidity in the experimental area underwent large fluctuations. This caused variable leakage drifts in the monitor circuit, which introduced an additional error in the absolute determination of the cross sections. For the polarization measurements, however, this did not matter. This was due to the fact that during the time of any given asymmetry measurement the drift was negligible. This was done by occasionally repeating the measurements of iron at 6.4°. It was found that the most probable maximum error introduced by this effect in the absolute values of the cross sections was about 10%. Because

[30] Aron, Hoffman, and Williams, U. S. Atomic Energy Commission Report AECU-663 (unpublished); University of California Radiation Laboratory Report UCRL-12, 1949 (unpublished).

TABLE II. Polarization and cross-section data for 424-Mev protons scattered from C, Al, Fe, and Ag. The angular resolution represents the total resolution as summarized in Table III. The errors are based on the variance of the counts from measurement to measurement. The polarization has in addition to the recorded errors, an absolute uncertainty of 0.9% due to the error in the initial polarized beam, and also a misalignment error which is summarized in Table IV. The cross section has in addition to the recorded errors, an absolute error of 2% in the initial calibration, and an absolute error due to the variable drift in the monitor of maximum 10%. However, the relative error for each element due to this drift is less than 5%. The cross section is expressed in barns/sterad, the polarization in percent, and the laboratory scattering angle in degrees.

θ^0	$(d\sigma/d\Omega)_{\text{left}}$	$(d\sigma/d\Omega)_{\text{right}}$	P
	Carbon		
5.7±0.8	0.754 ±0.063	0.536 ±0.013	31.8± 9.3
6.4±0.8	0.621 ±0.021	0.428 ±0.027	34.4± 6.0
7.6	0.461 ±0.004	0.326 ±0.009	32.0± 2.2
8.3	0.384 ±0.016	0.271 ±0.005	32.5± 4.9
9.0	0.313 ±0.011	0.203 ±0.002	40.0± 3.9
9.8	0.239 ±0.004	0.143 ±0.008	47.3± 4.1
10.4	0.223 ±0.007	0.131 ±0.007	48.8± 5.4
11.6	0.116 ±0.006	0.072 ±0.002	44.3± 5.8
12.3	0.0831±0.0039	0.0610±0.0035	28.6± 7.7
13.9	0.0322±0.0007	0.0285±0.0006	11.6± 3.0
14.8	0.0147±0.0010	0.0152±0.0007	−(3.2± 7.7)
15.9	0.0069±0.0005	0.0095±0.0006	−(30.0± 9.3)
18.5	0.0022±0.0002	0.0027±0.0002	−(18.5±12.5)
20.0	0.0030±0.0002	0.0024±0.0002	19.3± 8.0
	Aluminum		
6.4±1.0	1.88 ±0.09	1.53 ±0.01	19.3± 5.0
8.3±1.0	0.774 ±0.023	0.634 ±0.011	18.5± 3.4
9.8	0.222 ±0.002	0.214 ±0.006	4.7± 2.8
10.4	0.189 ±0.002	0.167 ±0.003	11.6± 2.4
11.6	0.0518±0.0021	0.0546±0.0031	−(4.8± 6.7)
12.3	0.0338±0.0026	0.0367±0.0021	−(7.9± 9.0)
13.5	0.0221±0.0009	0.0207±0.0052	6.0± 2.4
13.9	0.0235±0.0017	0.0176±0.0009	27.1± 9.0
14.8	0.0227±0.0011	0.0108±0.0004	67.1± 7.1
15.9	0.0294±0.0011	0.0130±0.0011	72.3± 6.9
18.5	0.0170±0.0009	0.0095±0.0006	52.7± 8.0
	Iron		
5.7±1.1	5.39 ±0.15	4.25 ±0.27	22.1± 6.0
6.4±1.1	3.16 ±0.06	2.34 ±0.02	27.7± 4.1
7.6	1.49 ±0.07	1.13 ±0.04	25.0± 5.6
8.3	0.579 ±0.021	0.473 ±0.014	18.9±12.5
9.0	0.359 ±0.024	0.277 ±0.007	24.1± 4.7
9.8	0.130 ±0.009	0.084 ±0.004	40.4±10.7
10.4	0.100 ±0.001	0.048 ±0.005	65.0± 8.8
11.6	0.123 ±0.007	0.0466±0.0032	84.1± 8.6
12.3	0.157 ±0.006	0.0704±0.0023	71.2± 5.4
12.8	0.150 ±0.003	0.0635±0.0043	75.5± 4.5
13.9	0.136 ±0.007	0.0647±0.0046	66.7± 8.0
15.9	0.0598±0.0029	0.0316±0.0020	57.2± 7.1
18.5	0.0135±0.0006	0.0109±0.0006	18.1± 5.4
	Silver		
5.7±1.0	4.71 ±0.50	5.20 ±0.03	−(9.2± 9.3)
6.4±1.0	2.52 ±0.11	2.86 ±0.07	−(11.6± 4.5)
7.6	0.379 ±0.048	0.407 ±0.042	−(6.9±15.1)
8.3	0.425 ±0.028	0.280 ±0.015	38.7± 8.4
9.0	0.400 ±0.027	0.237 ±0.021	47.7± 8.4
9.8	0.397 ±0.040	0.215 ±0.065	55.5±14.8
10.4	0.539 ±0.033	0.269 ±0.022	62.4± 9.0
11.6	0.263 ±0.014	0.162 ±0.006	44.5± 6.7
12.3	0.237 ±0.015	0.167 ±0.014	32.3± 9.9
12.8	0.118 ±0.006	0.0920±0.0047	23.0± 6.5
13.9	0.0472±0.0059	0.0554±0.0047	−(14.8±14.2)
14.8	0.0519±0.0118	0.0283±0.0083	54.6±32.9
15.9	0.0425±0.0059	0.0165±0.0035	81.7±22.4
18.5	0.0295±0.0035	0.0177±0.0012	50.5±16.8
19.2	0.0165±0.0024	0.0141±0.0024	15.0±18.7

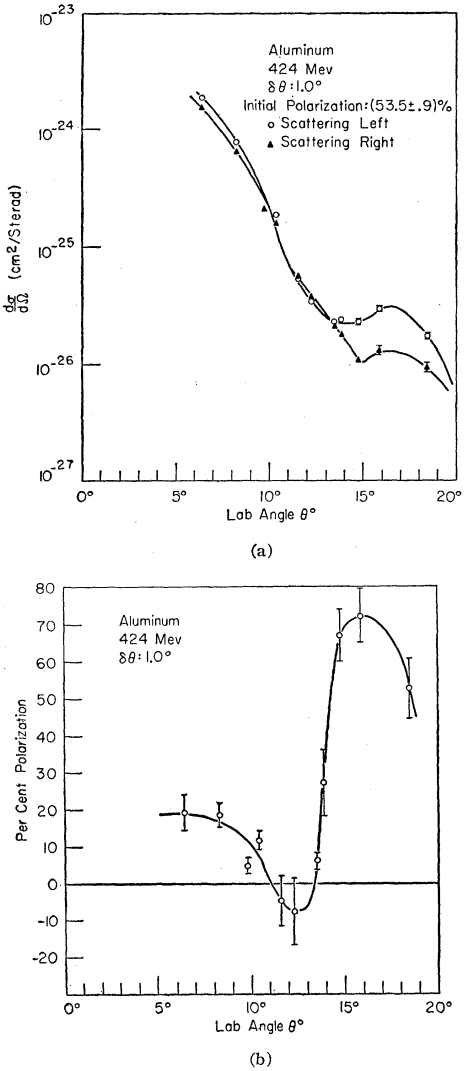

FIG. 6. (a) Differential cross-section curves for 424-Mev protons scattered left and right from aluminum. (b) Corresponding polarization curves for 424-Mev protons scattered from aluminum.

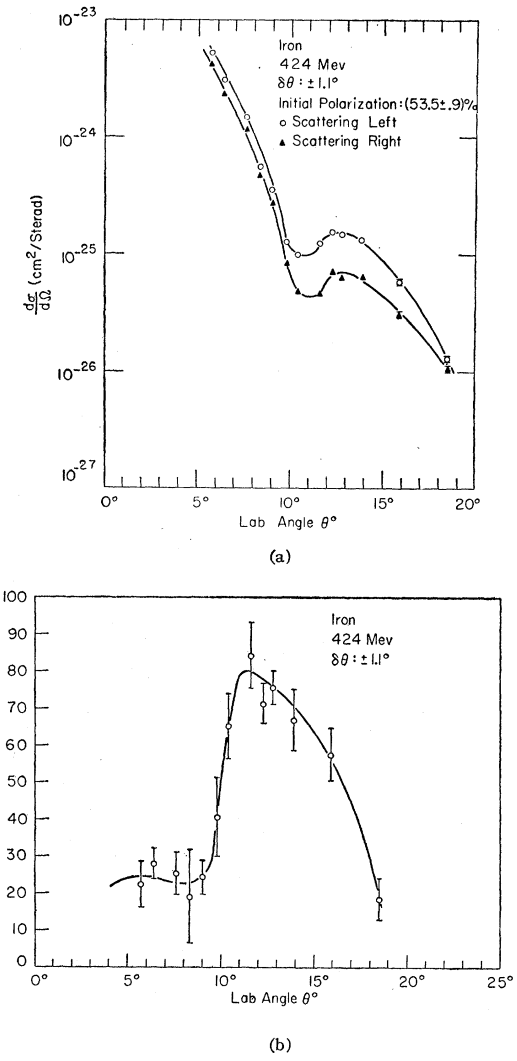

FIG. 7. (a) Differential cross-section curves for 424-Mev protons scattered left and right from iron. (b) Corresponding polarization curve for 424-Mev protons scattered from iron.

of the shorter time involved in recording the data for one target, the relative error for each element due to this drift was smaller (<5%).

B. Angular Resolution

The total angular resolution was determined by the multiple scattering, the divergence of the beam, the width of the target, and the width of the defining counter. Table III indicates how these factors are folded in to give the final resolution.

The resolution is most precisely determined experimentally. With the present geometry, however, it was an extremely difficult thing to do. This is essentially because the beam was broader than the target. Nevertheless, similar work in Berkeley[3] reveals that good agreement exists between angular resolutions calculated and found experimentally.

C. Misalignment Error

It can be shown[31] if e^2 is much less than one, that an angular misalignment ($\Delta\theta$) of the scattering table introduces the following maximum error (ΔP) in the polarization:

$$\Delta P = \left(\frac{d \ln(d\sigma/d\Omega)_0}{d\theta}\right)\Delta\theta, \qquad (2)$$

where $(d\sigma/d\Omega)_0$ is the average differential cross section of the "left" and "right" measurements at one angle.

If one assumes a misalignment of 0.07°, formula (2) gives the maximum error introduced to the polarization for the different targets as exhibited in Table IV.

[31] R. D. Tripp, University of California Radiation Laboratory Report UCRL-2075, April, 1955 (unpublished).

D. Cross-Section Results

The relationship between counts per monitor cycle (I) and the differential cross section in the laboratory system ($d\sigma/d\Omega$), is given by the following expression:

$$I = n\,\Delta\Omega\,Nl(1-e^{-t/l})(d\sigma/d\Omega), \qquad (3)$$

where n is the number of protons hitting the target during a monitoring cycle, N is the number of scattering nuclei/cc, t is the thickness of the target, $\Delta\Omega$ is the subtended solid angle, and l is the mean free path, which was calculated for the different elements by means of the total cross sections found by Nedzel[32] and de Carvalho.[29]

In a previous run with 431-Mev protons, the average differential cross section for iron at a scattering angle of $(5.8\pm0.7)°$, was found to be (4.56 ± 0.09) barns/sterad. The error is based on the counting statistics. Unfortunately, the energy threshold of the telescope in this geometry was set just above the knee of the corresponding range curve. This is a lower energy threshold than employed in the present run. As most of the scattering is elastic at small angles, it is felt justified to use this measurement as a scaling point for all the cross sections in the present experiment. By scaling this value by the ratio of the De Broglie wavelengths, the above reference point is found to be (4.60 ± 0.09) barns/sterad.

In order to determine the cross sections for the three other elements, the product $n\times\Delta\Omega$ in Eq. (3) has to be accurately known. Because of the geometry used, this factor is the same for all the targets. By inserting the above cross-section value for iron together with the corresponding measured counting rate (I) in Eq. (3), the product is readily obtained.

TABLE III. Total angular resolution for the various targets used. $(\theta_{\text{rms}}{}^0)^2$ is the contribution due to multiple scattering. The contribution due to the widths of the target and the defining counter is $(\theta_{\text{geom}}{}^0)^2=0.15$. The total resolution includes also the divergence of the beam (0.6°).

Element	Thickness (g/cm²)	Width (in.)	$(\theta_{\text{rms}}{}^0)^2$	Total angular resolution
C	2.22	0.705 in.	0.14	0.8°
Al	3.58	0.706 in.	0.41	1.0°
Fe	3.67	0.705 in.	0.74	1.1°
Ag	1.68	0.711 in.	0.55	1.0°

TABLE IV. The maximum error in the polarization measurements due to angular misalignment, which was estimated to be $\Delta\theta=0.07°$.

Element	$\left[\frac{d\ln(d\sigma/d\Omega)_\theta}{d\theta}\right]_{\max}$	$\Delta P(\%)$
C	0.7	1.0
Al	1.1	1.5
Fe	1.4	2.0
Ag	3.3	4.5

[32] V. A. Nedzel, Phys. Rev. 94, 174 (1954).

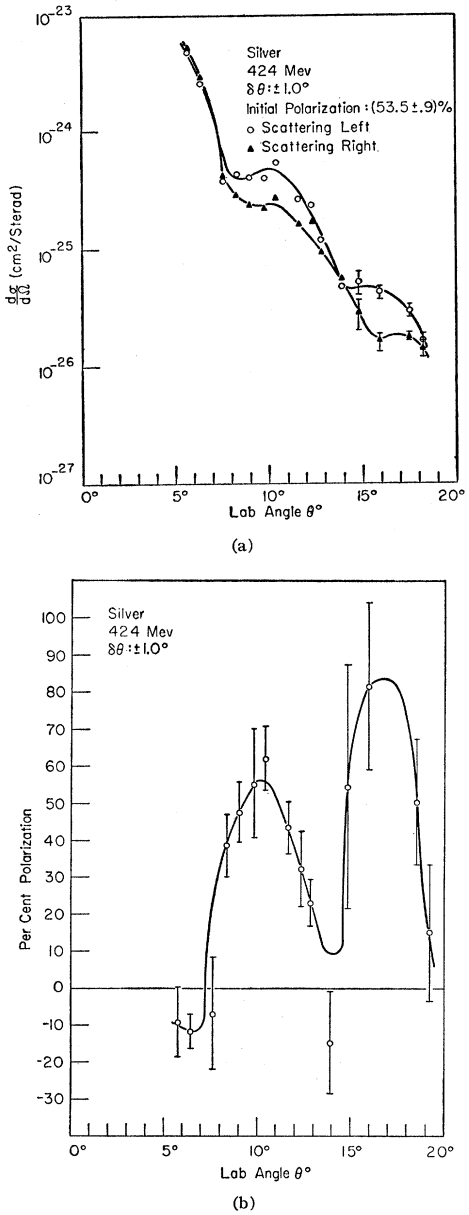

FIG. 8. (a) Differential cross-section curves for 424-Mev protons scattered left and right from silver. (b) Corresponding polarization curve for 424-Mev protons scattered from silver.

Figure 5(a) gives also a comparison with Chesnut's[2] cross-section curves for carbon. His average cross-section values seem to be lower than the present.

E. Polarization Results

The present data exhibit stronger angular variations in the polarization curves than seen in most previous work. The reason is that in this experiment more inelastic scattering has been filtered out of the elastic scattered beam. A comparison with Chesnut's carbon data [Fig. 5(b)] indicates that the scattering in the

TABLE V. Total elastic cross sections for C, Al, Fe, and Ag. The experimentally found differential cross-section curves were extrapolated to zero degrees by means of the Fernbach, Serber, and Taylor optical model of the nucleus. Because of the uncertainties involved in the matching procedure, no errors are quoted. r_0 is assumed to be 1.2×10^{-13} cm. The cross sections are given in barns.

Element	$\sigma_{424\ \mathrm{Mev}}$	$\sigma_{340\ \mathrm{Mev}}{}^{\mathrm{Calif.}}$	$\sigma_{424}/\sigma_{\mathrm{geom}}$
C	0.053	0.098	0.22
Al	0.124	0.201	0.30
Fe	0.321	···	0.49
Ag	0.490	0.884	0.49

present case essentially leads to the ground state. On the grounds of the employed energy threshold, this was anticipated.

Strauch[8] measured the polarization of carbon at the first peak in the polarization curve as a function of energy. An extrapolation of his curve to 424 Mev shows that agreement exists between Chesnut's value and the present data.

It should be pointed out that carbon has an advantage over the other elements investigated, in the sense that its first excited state is 4.4 Mev above the ground state, the second 7.5 Mev, the third 9.6 Mev, and so on. The energy state density for the other elements is considerably higher, and the first level for all of them is less than 1 Mev. With the present experimental arrangement, it appears to be impossible to make any reasonable separation of the excited states involved in the scattering by these latter elements.

A further confirmation of the importance of good energy resolution is given in the "triples" data. For small angles, up to about the first diffraction minimum, the cross section and the polarization measurements of the "triples" are essentially in agreement with that of the "quadruples." At larger angles the "dips" and "peaks," which are so pronounced in the "quadruples," are more smeared out in the "triples."

F. Coulomb Interference

An inflection point is observed in Chesnut's polarization curve [Fig. 5(b)] at a scattering angle of about 8°. The inflection seems to be more pronounced at 137 Mev, as recently reported by a Harwell group.[6] It is also observed in the present data.

These "irregularities" can probably be explained on the basis of a Coulomb nuclear interference.[18,20–25,27] For elements of intermediate atomic number, the interference apparently results in a decrease of the maximum polarization and a broadening in the region of the dip. This might explain the initial shape of the polarization curves for aluminum [Fig. 6(b)] and iron [Fig. 7(b)]. In the case of silver [Fig. 8(b)], the interference is probably obscured because of the occurrence of the first diffraction minimum at a smaller angle.

A more quantitative formulation of this effect will be given in Sec. V.

G. Total Elastic Cross Section

As previously mentioned, 5.7° was the smallest scattering angle used in this experiment. By extrapolating the measured cross section curves to zero degrees, the total elastic cross sections for the various elements can be estimated. However, as the major contribution to this total cross section is from angles less than six degrees, the final result is extremely sensitive to how the extrapolation is made.

The Fernbach, Serber, and Taylor optical model of the nucleus[33] was employed for this purpose. Here the differential cross section is directly related to a first-order Bessel function as shown in Eq. (4):

$$\frac{d\sigma}{d\Omega}\sim\left(\frac{J_1((2kR\sin(\theta/2))}{2kR\sin(\theta/2)}\right)^2. \tag{4}$$

The results of the integrations are given in Table V. Because of the large uncertainties involved in the matching procedure, no errors are quoted. Table V gives a comparison with similar measurements done in Berkeley at 340 Mev.[34]

If any significance can be attached to a comparison of these two sets of measurements, a possible reason for the lower total elastic cross sections at higher energy is a corresponding increase in the transparency of the nucleus.

H. Nuclear Radius

A nuclear radius can be derived from the position of the first diffraction minimum in the average differential cross section curves. The final result, however, depends on the nuclear model chosen.

The Fernbach, Serber, and Taylor optical model of the nucleus[33] as expressed in Eq. (4), and a model based on the Born approximation were employed. The latter gives essentially a first-order spherical Bessel function, $j_1(2kR\sin(\theta/2))$, as the governing relationship between the differential cross section and the scattering angle.[12] The results of these two approaches are given in Table VI. The first model gives 1.03×10^{-13}

TABLE VI. Summary of nuclear radii for C, Al, Fe, and Ag determined by the location of the first diffraction minima in the average differential cross-section curves. A comparison is made between the Fernbach, Serber, and Taylor optical model of the nucleus and the Born approximation with the use of a real and an imaginary potential. r_0 is expressed in units of 10^{-13} cm, and the scattering angle (θ) in degrees.

Element	First diffr. min (θ)	r_0 (opt. model)	r_0 (Born appr.)
C	18.7	0.98	1.15
Al	14.4	1.03	1.20
Fe	10.7	1.07	1.25
Ag	9.0	1.04	1.23

[33] Fernbach, Serber, and Taylor, Phys. Rev. **75**, 1352 (1949).
[34] Richardson, Ball, Leith, and Moyer, Phys. Rev. **86**, 29 (1952).

cm for the average nuclear radius, which agrees with what a Berkeley group obtained at 340 Mev on the basis of the same model. The Born approximation gives 1.2×10^{-13} cm.

As is well known, the determination of nuclear radii depends very much upon the particular nature of the experiment performed and the model used. In this case, the Born approximation tends to give a more consistent radius with the total cross section results of Nedzel[32] and de Carvalho.[29]

V. THEORIES OF POLARIZATION, FINAL DISCUSSION OF RESULTS

At present, a detailed theoretical fit to Chesnut's data[2] has not appeared. A theoretical analysis of the reported data is further complicated by the number of excited states involved. It is, therefore, felt justified to limit this section to a qualitative comparison of the data with the existing approaches.

Accurate analysis based on phase shifts[13,15,18–27] involves long and tedious calculations, which obscures the physics of the problem. The Born approximation is in general rather inadequate, but gives a much better indication of the mechanism involved in high-energy polarization.[13,16,17] A general outline of the Born approximation will therefore now be given.

Here the nucleus is considered as a whole and being represented by a potential, assumed to consist of four parts:

$$V=V_c+V_1+i(V_a+V_s). \tag{5}$$

V_1 is real, and generally assumed to be a square well; $i(V_a+V_s)$ is the imaginary contribution to the total potential, where V_a represents in the usual fashion the absorption properties of the nuclear matter[33] and V_s is the spin-dependent term normally of the same type as the Thomas correction;[13] V_c is the electrostatic potential of the nucleus. Because of the charge distribution,[35] it is not correct to assume a point charge, but for this rough estimate it should not matter.

With these assumptions, the Born approximation gives the following expressions for the asymmetry and the differential cross section.

$$\epsilon=\frac{15\eta^2(V_a/V_1)\sin\theta(\boldsymbol{\sigma}\cdot\mathbf{n})}{\left(\frac{R^2}{r_0{}^6Q^2V_1{}^2}-1\right)^2+\left(\frac{V_a}{V_1}\right)^2+\frac{225}{4}\eta^4\sin^2\theta(\boldsymbol{\sigma}\cdot\mathbf{n})}. \tag{6}$$

$$\frac{d\sigma}{d\Omega}=\frac{4M^2}{\hbar^4}r_0{}^6Q^2V_1{}^2\left[\left(\frac{R}{r_0{}^3QV_1}-1\right)^2+\left(\frac{V_a}{V_1}+\frac{15}{2}\eta^2\sin\theta\right)^2\right], \tag{7}$$

where

$$R=\frac{Ze^2}{(P/\hbar)^2+(1/r_0)^2};\quad Q=\frac{\sin q}{q^3}-\frac{\cos q}{q^2};\quad \eta=\frac{P}{Mc}.$$

All the notations have their standard meanings.[12,13]

For the forward scattering angles these formulas roughly describe the scattering. The qualitative statement made about the Coulomb interference, in Sec. IV E, is quantatively expressed in Eq. (6). However, the oscillatory trends found in the reported polarization curves at angles corresponding to the diffraction minima are not displayed in the Born approximation.

In the more detailed phase shift analysis, the following parameters are usually varied, the shape and the depth of the real and imaginary potentials, and the strength of the spin-orbit interaction, which frequently is split up into a real and an imaginary part.[27] A better agreement with the experimentally observed polarization data is in this way achieved.

VI. ACKNOWLEDGMENTS

The author is indebted to J. Marshall and L. Marshall for suggesting the problem, and for their valuable guidance throughout the experiment. J. Friedman and F. Solmitz have been very helpful in discussing the data. Much advice has been received from J. Fischer in the operation of the electronics and in the design of the equipment. H. Kobrak's active cooperation in assisting with the equipment and the data-recording is very much appreciated. Thanks go further to the machine shop, the cyclotron crew and operators, and many other members of this Institute who in one phase or the other have been involved in the experiment.

Finally, the author wants to express gratefulness to relatives in Norway and Sweden, who indirectly have supported his training at the University of Chicago.

[35] E. E. Chambers and R. Hofstadter, Phys. Rev. **103**, 1454 (1956); J. A. McIntyre, Phys. Rev. **103**, 1464 (1956).